Growth of Oriented Single-Crystalline Rutile TiO₂ Nanorods on Transparent Conducting Substrates for Dye-Sensitized Solar Cells

Bin Liu and Eray S. Aydil*

Department of Chemical Engineering and Materials Science, University of Minnesota, 421 Washington Avenue SE, Minneapolis, Minnesota 55455

Received October 6, 2008; E-mail: aydil@umn.edu

Abstract: Dye-sensitized solar cells (DSSCs) made from oriented, one-dimensional semiconductor nanostructures such as nanorods, nanowires, and nanotubes are receiving attention because direct connection of the point of photogeneration with the collection electrode using such structures may improve the cell performance. Specifically, oriented single-crystalline TiO₂ nanorods or nanowires on a transparent conductive substrate would be most desirable, but achieving these structures has been limited by the availability of synthetic techniques. In this study, a facile, hydrothermal method was developed for the first time to grow oriented, single-crystalline rutile TiO₂ nanorod films on transparent conductive fluorine-doped tin oxide (FTO) substrates. The diameter, length, and density of the nanorods could be varied by changing the growth parameters, such as growth time, growth temperature, initial reactant concentration, acidity, and additives. The epitaxial relation between the FTO substrate and rutile TiO₂ with a small lattice mismatch plays a key role in driving the nucleation and growth of the rutile TiO₂ nanorods on FTO. With TiCl₄-treatment, a light-to-electricity conversion efficiency of 3% could be achieved by using 4 μm-long TiO₂ nanorod films as the photoanode in a DSSC.

Introduction

Synthesis of aligned single-crystalline wide bandgap semiconductor nanorod or nanowire films has attracted much attention because of their potential applications in novel photovoltaic devices including ordered hybrid bulk heterojunction as well as dye- and quantum-dot-sensitized solar cells.[1−8]

Single crystal nanorods or nanowires offer direct electrical pathways for photogenerated electrons and could increase the electron transport rate, which in turn may improve the performance of photovoltaic devices such as dye-sensitized solar cells (DSSCs).[2−8] To date, most of the one-dimensional nanostructured DSSCs have been limited to single-crystalline ZnO nanorods/nanowires[2,3] or polycrystalline TiO₂ nanowires or nanotubes[5−7] by the existing available synthetic techniques. Owing primarily to the instability of ZnO in acidic dye solution, the DSSCs assembled from ZnO show poor performance compared to those made from TiO₂.[9] One-dimensional polycrystalline TiO₂ nanostructures (either nanowires or nanotubes) still have electron scattering or trapping at grain boundaries and show only marginally improved electron transport rate in DSSCs.[5−7]

Single-crystalline TiO₂ nanorod or nanowire films would be preferred over polycrystalline ones for use in ordered bulk heterojunction as well as in DSSCs. Unlike ZnO, crystal structure and symmetry of TiO₂ (either anatase or rutile) make the growth of oriented anisotropic single-crystalline TiO₂ films very difficult. To date, there are only a few reports that describe heterogeneous growth of oriented single-crystalline TiO₂ nanorods or nanowires.[10−14] None are on transparent conducting substrate, a prerequisite for fabrication of solar cells. In addition, most heterogeneous growth methods used to date relied on vapor phase syntheses. Compared to vapor phase techniques, solution-

(1) (a) Huang, M. H.; Mao, S.; Feick, H.; Yan, H. Q.; Wu, Y. Y.; King, H.; Weber, E.; Russo, R.; Yang, P. D. *Science* **2001**, *292*, 1897–1899. (b) Xia, Y. N.; Yang, P. D.; Sun, Y. G.; Wu, Y. Y.; Mayers, B.; Gates, B.; Yin, Y. D.; Kim, F.; Yan, Y. Q. *Adv. Mater.* **2003**, *15*, 353–389. (c) Greene, L. E.; Law, M.; Goldberger, J.; Kim, F.; Johnson, J. C.; Zhang, Y.; Saykally, R. J.; Yang, P. D. *Angew. Chem., Int. Ed.* **2003**, *42*, 3031–3034. (d) Greene, L. E.; Law, M.; Tan, D. H.; Montano, M.; Goldberger, J.; Somorjai, G.; Yang, P. D. *Nano Lett.* **2005**, *5*, 1231–1236. (e) Tian, Z. R.; Voigv, J. A.; Liu, J.; Mckenzie, B.; Xu, H. F. *J. Am. Chem. Soc.* **2003**, *125*, 12384–12385. (f) Vayssieres, L.; Graetzel, M. *Angew. Chem., Int. Ed.* **2004**, *43*, 3666–3670.

(2) (a) Law, M.; Greene, L. E.; Johnson, J. C.; Saykally, R. J.; Yang, P. D. *Nat. Mater.* **2005**, *4*, 455–459. (b) Law, M.; Greene, L. E.; Radenovic, A.; Kuykendall, T.; Liphardt, J.; Yang, P. D. *J. Phys. Chem. B* **2006**, *110*, 22652–22663. (c) Greene, L. E.; Yuhas, B. D.; Law, M.; Zitoun, D.; Yang, P. D. *Inorg. Chem.* **2006**, *45*, 7535–7543.

(3) (a) Baxter, J. B.; Aydil, E. S. *Appl. Phys. Lett.* **2005**, *86*, 053114. (b) Baxter, J. B.; Walker, A. M.; van Ommering, K.; Aydil, E. S. *Nanotechnology* **2006**, *17*, S304–S312.

(4) (a) Greene, L. E.; Law, M.; Yuhas, B. D.; Yang, P. D. *J. Phys. Chem. C* **2007**, *111*, 18451–18456. (b) Takanezawa, K.; Hirota, K.; Wei, Q.-S.; Tajima, K.; Hashimoto, K. *J. Phys. Chem. C* **2007**, *111*, 7218–7223. (c) Olson, D. C.; Shaheen, S. E.; Collins, R. T.; Ginley, D. S. *J. Phys. Chem. C* **2008**, *112*, 9544–9547.

(5) Mor, G. K.; Shankar, K.; Paulose, M.; Varghese, O. K.; Grimes, C. A. *Nano Lett.* **2006**, *6*, 215–218.

(6) Zhu, K.; Neale, N. R.; Miedaner, A.; Frank, A. J. *Nano Lett.* **2007**, *7*, 69–74.

(7) Enache-Pommer, E.; Boercker, J. E.; Aydil, E. S. *Appl. Phys. Lett.* **2007**, *91*, 123116.

(8) Leschkies, K. S.; Divakar, R.; Basu, J.; Enache-Pommer, E.; Boercker, J. E.; Carter, C. B.; Kortshagen, U. R.; Norris, D. J.; Aydil, E. S. *Nano Lett.* **2007**, *7*, 1793–1798.

(9) Keis, K.; Magnusson, E.; Lindstrom, H.; Lindquist, S. E.; Hagfeldt, A. *Sol. Energy Mater. Sol. Cells* **2002**, *73*, 51–58.

based methods are more suitable for inexpensive mass production. In this article, we describe a simple hydrothermal method for growing oriented, single-crystalline rutile TiO_2 nanorods on FTO substrates. Rutile TiO_2 has been proven to be comparable to anatase TiO_2 in DSSCs with additional advantages including better chemical stability and higher refractive index.[15,16]

Experimental Section

In a typical synthesis, 0−60 mL of deionized water was mixed with 0−60 mL of concentrated hydrochloric acid (36.5%−38% by weight) to reach a total volume of 60 mL in a Teflon-lined stainless steel autoclave (125 mL volume, Parr Instrument Co.). The mixture was stirred at ambient conditions for 5 min before the addition of 1 mL of titanium butoxide (97% Aldrich). After stirring for another 5 min, two pieces of FTO substrates (F:SnO_2, Tec 15, 10 Ω/□, Hartford Glass Company), ultrasonically cleaned for 60 min in a mixed solution of deionized water, acetone, and 2-propanol with volume ratios of 1:1:1, were placed at an angle against the wall of the Teflon-liner with the conducting side facing down. The hydrothermal synthesis was conducted at 80−220 °C for 1−24 h in an electric oven. After synthesis, the autoclave was cooled to room temperature under flowing water, which took approximately 15 min. The FTO substrate was taken out, rinsed extensively with deionized water and allowed to dry in ambient air. In some control experiments, ultrasonically cleaned silicon or glass substrates were used instead of FTO to study the effect of the substrate. Effects of additional titanium precursors such as titanium isopropoxide or titanium tetrachloride (TiCl_4) as well as effects of adding surfactants or salts such as ethylenediamine (EDA), ethylenediaminetetraacetic acid (EDTA), sodium dodecyl sulfate (SDS), cetyltrimethylammoniumbromide (CTAB), polyvinylpyrrolidone (PVP), sodium chloride (NaCl) were also studied.

The crystal structure of the as-prepared film was examined by X-ray diffraction (XRD). The XRD patterns were recorded in a Bruker-AXS Microdiffractometer (model D5005) with Cu Kα radiation ($\lambda = 1.5406$ Å) from 20° to 70° at a scanning speed of 2.4° min^{-1}. X-ray tube voltage and current were set at 45 kV and 40 mA, repectively. Morphological and lattice structural information were examined with field emission scanning electron microscopy (FESEM, JSM-6500F, and JSM-6700F), transmission electron microscopy (TEM/HRTEM, FEI Tecnai G2 30), and selected area electron diffraction (SAED). In a typical FESEM measurement, a small piece of sample film was adhered onto a copper stub using double-sided carbon tape. The specimens for TEM imaging were prepared by suspending solid samples in acetone. About 1−2 mg of white sample detached from the FTO substrate was added to 5 mL of acetone in a small glass vial, followed by sonication for 30 min. A few drops of the sonicated suspension were dropped onto a carbon-coated 200 mesh copper grid and dried under ambient conditions before imaging.

Dye-sensitized solar cells were assembled using the TiO_2 nanorods grown on FTO as the photoanode. Prior to dye adsorption, the as-prepared sample was placed in 100 mL of 0.1 M TiCl_4
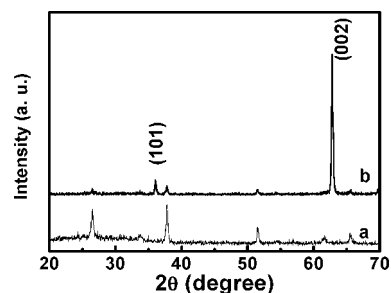

Figure 1. XRD patterns of the FTO substrate (a) before hydrothermal growth and (b) after hydrothermal growth.

solution, which was prepared by mixing TiCl_4 and ice, at 50 °C for 1 h in a beaker covered with parafilm. After rinsing with pure ethanol, the TiCl_4-treated sample was annealed in air at 450 °C for 30 min inside a furnace. The sensitizer used in this work was *cis*-bis(isothiocyanato)bis(2,2′-bipyrridyl-4-4′-dicarboxylato)-ruthenium(II)bis-tetrabutylammonium dye (N-719 as received from Solaronix); the nanorod samples were immersed in a 0.3 mM ethanolic solution of N-719 for 24 h to complete the dye adsorption. A platinum-coated FTO substrate spaced from the TiO_2 nanorod photoanode with 25-μm thick Teflon strips (Pike Technologies) was used as the counter electrode. The electrolyte containing 0.6 M 1-butyl-3-methylimidazolium iodide, 0.03 M I_2, 0.5 M *tert*-butylpyridine, and 0.1 M guanidinium thiocyanate in acetonitrile/valeronitrile 85/15 (v/v) (ES-004 from Iolitec) was injected into the space between the anode and the cathode through capillary forces.

The current−voltage characteristics were recorded with a Keithley 2400 sourcemeter using a simulated AM1.5 spectrum produced by a homemade solar simulator described in a previous publication.[17] Briefly, the measurement system consisted of a 100 W Xe-arc lamp (Oriel) in conjunction with a 0.125 m monochromator (Newport, Cornerstone 130) equipped with a grating and a mirror mounted on the same turret. AM1.5 radiation was simulated using two filters (Newport 81090 and 81092) placed between the monochromator and the Xe lamp and by selecting the mirror on the grating turret. The photoaction spectrum, $I(\lambda)$ was acquired by selecting and scanning the grating. The lamp irradiance, $P(\lambda)$, was recorded using two independent methods, a calibrated radiometry system consisting of a silicon detector and a power meter (International Light SED033 and IL1700) and a Newport radiant power meter (Newport 70260 and 70268 probe) that agreed with each other. The lamp power was adjusted such that the measured integrated irradiance was approximately 100 mW/cm^2. The external quantum efficiency was calculated using $EQE(\lambda) = (hc/\lambda) \times [I(\lambda) - I_{dark}]/P(\lambda)$, where $I(\lambda)$ and I_{dark} is the short-circuit current recorded under illumination and in the dark, respectively. No corrections were made for reflection from the glass substrate, and the solar cell area was defined with a 0.33 cm^2 circular aperture.

Results and Discussion

XRD shows that the films deposited on FTO substrates are rutile TiO_2. Figure 1 displays the XRD patterns of the FTO substrate before and after the hydrothermal reaction. All the diffraction peaks that appear upon nanorod growth agree well with the tetragonal rutile phase (SG, $P4_2/mnm$; JCPDS No. 88−1175, $a = b = 0.4517$ nm and $c = 0.2940$ nm). Compared to the powder diffraction pattern, the (002) diffraction peak was significantly enhanced, and some diffraction peaks including (110), (111), and (211) were absent, which indicates that the as-deposited film is highly oriented with respect to the substrate

(10) Wu, J.-J.; Yu, C.-C. *J. Phys. Chem. B* **2004**, *108*, 3377−3379.
(11) (a) Wu, J.-M.; Shih, H. C.; Tseng, Y.-K.; Hsu, C.-L.; Tsay, C.-Y. *J. Electrochem. Soc.* **2007**, *154*, H157−H160. (b) Wu, J.-M.; Shih, H. C.; Wu, W.-T. *Nanotechnology* **2005**, *17*, 105−109.
(12) Chen, C. A.; Chen, Y. M.; Korotcov, A.; Huang, Y. S.; Tsai, D. S.; Tiong, K. K. *Nanotechnology* **2008**, *19*, 075611.
(13) Weng, C.-C.; Hsu, K.-F.; Wei, K.-H. *Chem. Mater.* **2004**, *16*, 4080−4086.
(14) (a) Hosono, E.; Fujihara, S.; Kakiuchi, K.; Imai, H. *J. Am. Chem. Soc.* **2004**, *126*, 7790−7791. (b) Kakiuchi, K.; Hosono, E.; Imai, H.; Kimura, T.; Fujihara, S. *J. Cryst. Growth* **2006**, *293*, 541−545. (c) Feng, X. J.; Zhai, J.; Jiang, L. *Angew. Chem., Int. Ed.* **2005**, *44*, 5115−5118.
(15) Kim, K. J.; Benksten, K. D.; van de Lagemaat, J.; Frank, A. J. *Chem. Mater.* **2002**, *14*, 1042−1047.
(16) Park, N.-G.; van de Lagemaat, J.; Frank, A. J. *J. Phys. Chem. B* **2000**, *104*, 8989−8994.

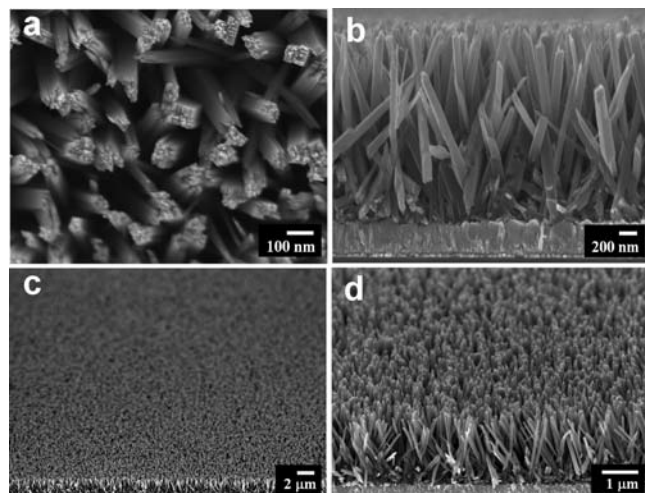(17) Boercker, J. E.; Enache-Pommer, E.; Aydil, E. S. *Nanotechnology* **2008**, *19*, 095604.

Figure 2. FESEM images of oriented rutile TiO_2 nanorod film grown on FTO substrate in 30 mL of deionized water, 30 mL of hydrochloric acid, and 1 mL of titanium butoxide at 150 °C for 20 h. (a) top view, (b) cross-sectional view, (c) and (d) tilted cross-sectional views.

Figure 3. (a) HRTEM image of a single TiO_2 nanorod shown in the inset; (b) SAED pattern of the same TiO_2 nanorod.

surface and the TiO_2 nanorods grow in the [001] direction with the growth axis parallel to the substrate surface normal. Absence of diffraction peaks that are normally present in polycrystalline or powder samples is a strong indication that the nanorods are not only aligned but are also single crystalline throughout their length. These conclusions were confirmed by HRTEM and SAED measurements (vide infra).

Figure 2 shows typical FESEM images of the nanorod film grown at 150 °C for 20 h. The images at different locations and magnifications reveal that the entire surface of the FTO substrate is covered very uniformly with TiO_2 nanorods. Top and side views in Figure 2 show that the top surface of the nanorods appears to contain many step edges, while the side surface is smooth. Growth appears to proceed by addition of titanium growth units (e.g., $[Ti(OH)_2Cl_2(OH)_2]^0)^{18}$ at the step edges. The nanorods are tetragonal in shape with square top facets, the expected growth habit for the tetragonal crystal structure. The nanorods are nearly perpendicular to the FTO substrate. After 20 h of growth, the average diameter and length, as determined from FESEM and TEM images, were 90 ± 5 nm and 1.9 ± 0.1 μm, respectively. The nanorods are single-crystalline, as evidenced by the sharp SAED pattern of a nanorod examined along the $[1\bar{1}0]$ zone axis (Figure 3b). Examination of individual nanorods with HRTEM shows that they are completely crystalline along their entire lengths. Lattice fringes with interplanar spacings, $d_{110} = 3.2 \pm 0.1$ Å and $d_{001} = 2.9 \pm 0.1$ Å are clearly imaged and are consistent with the rutile phase. The [110] axis is perpendicular to the nanorod side walls, and the nanorods grow along the [001] direction, consistent with the XRD data. The chemical stoichiometry of the nanorods was further examined with EDX. and the atomic ratio of Ti to O was found to be ∼1:2 (Supporting Information, SI-1).

Effect of Growth Time. The FTO substrate remained transparent, and no TiO_2 nanorods were observed when the growth time was less than 3 h at 150 °C. After 3 h, TiO_2 nanorods begin to grow on the FTO substrate with the rod axis aligned approximately perpendicular to the substrate. Those nanorods that nucleate and grow with their axis significantly misoriented
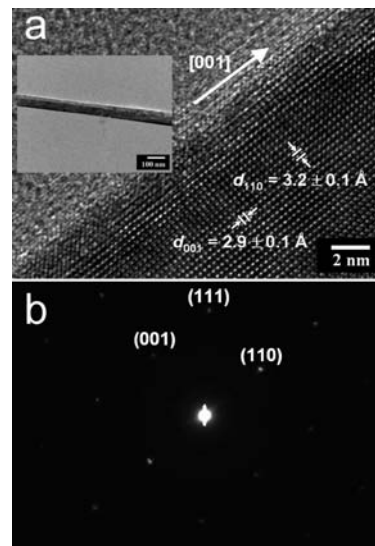
with respect to the substrate surface normal eventually collide with a neighboring nanorod and stop growing. The diameter quickly reaches 90 nm and remains constant with time even though the nanorods grow taller (Supporting Information, SI-2). The average nanorod length was 600 nm after 4 h of growth and increased to 2 μm after 20 h of growth. If the growth time is extended to over 24 h, a white film composed of aligned TiO_2 nanorods starts to peel off the FTO substrate. This white, paperlike film (Supporting Information, SI-2) could easily be collected, dried, and handled by a tweezer and can be transferred to an arbitrary second substrate while maintaining its microscopic structure.[19−21] The peeling of the film could be due to a competition between crystal growth and dissolution; at short reaction times, the supersaturation of the titanium salt is high, and nanorods grow. When the growth is carried out for longer times, the crystal growth rate starts to decrease as the system approaches equilibrium. At this point, crystal dissolution on high-energy surfaces such as the FTO−nanorod surface can become important. Indeed, this interface is strained due to the lattice mismatch between the FTO and the rutile nanorods and can dissolve even though the rest of the nanorod film is in equilibrium with the solution. After the TiO_2 nanorod film is lifted off the substrate, the substrate remains conductive which indicates that the film is peeling off at the FTO−nanorod interface.

At first it may appear that the TiO_2 nanorod film peeling off the substrate is a significant disadvantage and may limit the applications of these nanorods. If the reaction is carried out for a long time (e.g., 24 h) and allowed to reach equilibrium, the TiO_2 nanorod films do peel off from the FTO substrate. However, if the reaction is stopped before reaching the reaction equilibrium (e.g., less than ∼20 h), peeling is not observed. Following, the TiO_2 nanorod film can be grown longer by placing the substrate (with the nanorods) in a fresh solution and continuing the growth. For example, we grew TiO_2 nanorod

(18) Pottier, A.; Chanéac, C.; Tronc, E.; Mazerolles, L.; Jolivet, J. P. *J. Mater. Chem.* **2001**, *11*, 1161–1121.

(19) Dürr, M.; Schmid, A.; Obermaier, M.; Rosselli, S.; Yasuda, A.; Nelles, G. *Nat. Mater.* **2005**, *4*, 607–611.

(20) Zhang, D. S.; Yoshida, T.; Minoura, H. *Adv. Mater.* **2003**, *15*, 814–817.

(21) Park, J. H.; Lee, T.-W.; Kang, M. G. *Chem. Commun.* **2008**, *25*, 2867–2869.

films that are as thick as 8 μm by changing the growth solution every 4 h. These films remained adhered to the FTO and did not peel off the substrate (Supporting Information, SI-3). In principle, the TiO$_2$ nanorod films can be grown to desired lengths by refreshing the growth solution before the reaction reaches equilibrium.

Effect of Growth Temperature. TiO$_2$ nanorods did not grow on the FTO substrates when the temperature was less than 100 °C. On the other hand, increasing the hydrothermal reaction temperature from 150 to 200 °C increased the growth rate by a factor of 5 (Supporting Information, SI-4). The average diameter of the nanorods grown at 200 °C was slightly smaller. At 200 °C, the film begins to peel off the substrate after 6 h of reaction, and the thickness of the free-standing film is comparable to that obtained at 150 °C. At 200 °C, the solution reaches equilibrium faster, and as a result, dissolution that causes the peeling of the film begins earlier.

Effect of Substrates. Oriented TiO$_2$ nanorod film could only be grown on FTO substrates. Experiments to grow TiO$_2$ nanorods on glass or silicon substrates were unsuccessful, indicating that nucleation and growth may require epitaxy on FTO crystals. In fact, the FTO substrate also has the tetragonal rutile structure, and the lattice mismatch between the tetragonal FTO ($a = b = 0.4687$ nm)[22] and rutile TiO$_2$ ($a = b = 0.4594$ nm)[23] is 2%. This small lattice mismatch may promote the epitaxial nucleation and growth of rutile TiO$_2$ nanorods on FTO although conclusive proof of this hypothesis would require a careful study of the FTO–nanorod interface using transmission electron microscopy. We base our hypothesis on three observations. First TiO$_2$ nanorod array could only be grown on FTO. Second, TiO$_2$ nanorods are firmly attached on the FTO substrate and could not be detached even with the aid of ultrasonication. Finally, when the FTO film is patterned by removing portions of it from the substrate by etching, the TiO$_2$ nanorod array could only be grown selectively on the remaining FTO film. It is possible to have epitaxial growth from a polycrystalline film with majority of the TiO$_2$ nanorods aligned nearly normal to the substrate because FTO films on glass are highly textured with grains aligned preferentially in the (200) direction. Nevertheless, not all grains are aligned, and a significant number of TiO$_2$ nanorods grow off normal angles to the substrate. These nanorods run into nearby nanorods and stop growing. Thus, only those nanorods with axis nearly aligned with the substrate normal continue growing and give the nanorod film the array-like appearance. Indeed, using a nanowire diameter of 90 nm and an areal density of 40 nanowires/μm^2, we calculate that nanowires cover only ~25% of the substrate surface and higher nanowire densities are possible. Thus, not all FTO grains give rise to nanowires that grow normal to the surface. Obviously, if our hypothesis of epitaxy is correct, one way to increase nanowire density would be to increase the texture of the FTO film.

Effect of Initial Reactant Concentration. The density of the nanorods could be varied by changing the initial titanium precursor concentration in the growth solution. Figure 4 shows that the density of the nanorods could be varied between ~4 to ~50 μm^{-2} by increasing the initial titanium butoxide in the growth solution from 0.5 to 1 mL. Further increase in the amount of titanium butoxide causes rapid hydrolysis and homogeneous
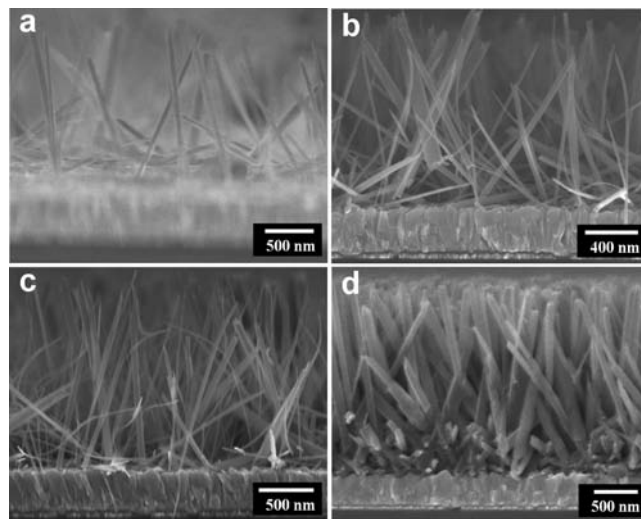
(22) Abd-Lefdil, M.; Diaz, R.; Bihri, H.; Aouaj, M. A.; Rueda, F. *Eur. Phys. J. Appl. Phys* **2007**, *38*, 217–219.
(23) Howard, C. J.; Sabine, T. M.; Dickson, F. *Acta Crystallogr., Sect. B* **1991**, *47*, 462–468.

Figure 4. FESEM images of oriented rutile TiO$_2$ nanorod films grown at 150 °C for 18 h with different amounts of titanium butoxide in a mixture of 30 mL of deionized water and 30 mL of hydrochloric acid; (a) 0.5 mL, (b) 0.75 mL, (c) 0.85 mL, and (d) 1 mL of titanium butoxide.

precipitation as soon as it is added to the growth solution. The growth solution remains turbid even after prolonged stirring, and the nanorods that grow under this condition are found to be covered by dendritic particles that have nucleated homogeneously and have settled on the nanorods film. It appears that when the titanium precursor concentration is low, the nanorods are not as aligned as those grown using higher titanium precursor concentrations. However, this appearance is a result of the changing nucleation density. When nucleation density is high, the nanorods growing at an angle to the substrate surface normal run into neighboring nanorods and stop growing (see for example shorter nanorods near the FTO surface in Figure 4d). On the other hand, when nucleation density is low, the nanorods at an angle can keep growing to longer lengths since the probability of running into a neighbor decreases. The nanorods can nucleate and grow at an angle to the substrate surface normal because the FTO is polycrystalline and its surface is rough. Thus, even though nanorods grow epitaxially, some FTO grains may be oriented such that nanorods grow at an angle to the substrate surface normal.

Effect of Acidity. The growth of TiO$_2$ nanorods on FTO substrate was favored when a mixed solution containing 30 mL of deionized water and 30 mL of hydrochloric acid was used. Increasing the volume of deionized water with respect to the volume of hydrochloric acid while keeping the total volume of the growth solution constant increased the hydrolysis rate of titanium butoxide. In fact, when titanium butoxide was introduced into 60 mL of deionized water, TiO$_2$ precipitated immediately. No nanorods were found on FTO substrate after hydrothermal growth in this solution. Thus, in the absence of hydrochloric acid or at low hydrochloric acid concentrations, all the titanium precursor precipitates and settles to the bottom of the reaction vessel as TiO$_2$, and none remains available for nanorod growth. Extremely low pH suppresses the hydrolysis of titanium butoxide. When a growth solution containing 15 mL of deionized water and 45 mL of hydrochloric acid was used, the solution remained clear after hydrothermal reaction, and TiO$_2$ did not form on the FTO substrate or in the homogeneous phase. Thus, we conclude that growth of oriented TiO$_2$ nanorods requires slow hydrolysis of titanium butoxide in a fairly strong acidic aqueous medium.
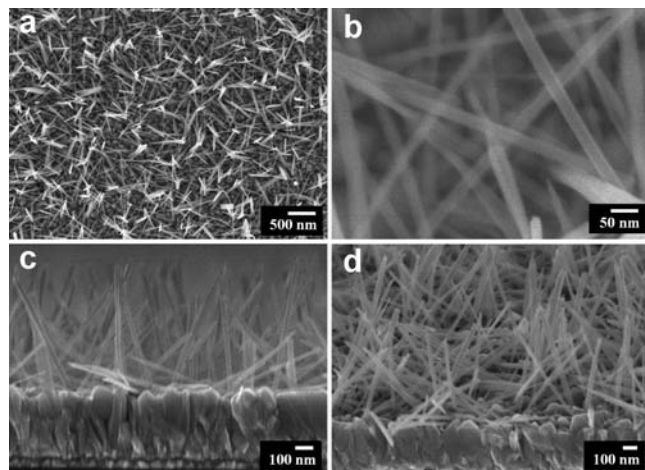
Figure 5. FESEM images of rutile TiO_2 nanorod films grown in 25 mL of deionized water, 5 mL of saturated aqueous NaCl solution, 30 mL of hydrochloric acid, and 1 mL of titanium butoxide at 150 °C for 8 h: (a) and (b) show the top view of the nanorods on two different scales; (c) shows the cross-sectional view of the nanorods, and (d) is the tilted cross-sectional view.

Effect of Titanium Precursors. The growth of oriented TiO_2 nanorod film on FTO is not restricted to titanium butoxide as the titanium source. Some common titanium salts such as titanium isopropoxide and titanium tetrachloride could also be utilized in this synthesis in lieu of titanium butoxide. The morphology of the nanorod film synthesized from titanium isopropoxide is similar to that synthesized from titanium butoxide (Supporting Information SI-5). When titanium tetrachloride was used as the titanium precursor, the diameter of the nanorods grew faster and reached an average value of 200 nm, possibly due to a higher chemical reactivity of $TiCl_4$ compared to other titanium precursors.

Effect of Adding Surfactants or Salts. The addition of some common surfactants or salts including EDA, EDTA, SDS, CTAB, and PVP had little effect on the morphology of TiO_2 nanorods (Supporting Information, SI-6). However, when growth was conducted by adding saturated aqueous NaCl solution to the growth solution, the density, alignment, and diameter of the nanorods could be changed. For example, Figure 5 shows that, when 5 mL of saturated aqueous NaCl solution was added to the growth solution, the density and diameter were both reduced to $\sim$40 μm^{-2} and $\sim$35 nm, respectively. The nanorods appear less aligned with the substrate surface normal because reduction of diameter and density decrease the probabilities of nanorods growing at an angle to substrate surface normal to stop growing by running into a neighbor. The exact role of NaCl in controlling the diameter and density of the nanorod growth is not fully understood, but several explanations are possible. First, addition of sodium chloride salt greatly increases the ionic strength of the growth solution,[24] and higher ionic strength favors the formation of smaller crystals through electrostatic screening.[25] Second, a layer of ions next to the nanorods can act as a diffusion barrier for the nanorod growth and retard the precursors from diffusing to the surface.[26] Finally,
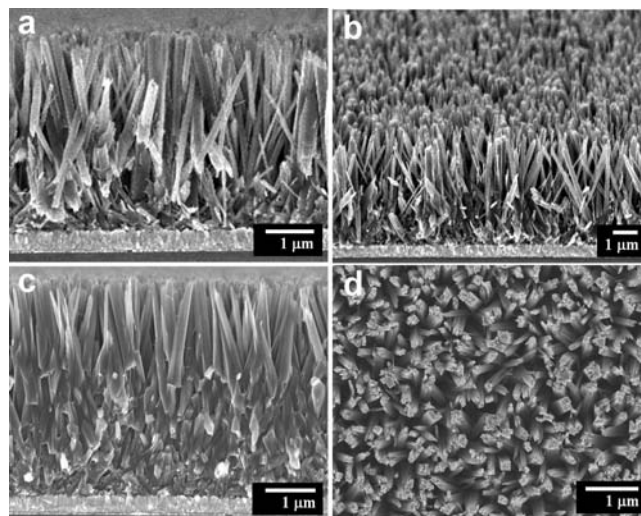
(24) Snoeyink, V. L.; Jenkins, D. *Water Chemistry*, 1st ed.; John Wiley & Sons: New York, 1980; Chapter 3, p 75.
(25) Vayssieres, L.; Chanéac, C.; Tronc, E.; Jolivet, J. P. *J. Colloid Interface Sci.* **1998**, *205*, 205–212.
(26) (a) Xu, R.; Zeng, H. C. *J. Phys. Chem. B* **2003**, *107*, 926–930. (b) Feng, J.; Zeng, H. C. *Chem. Mater.* **2003**, *15*, 2829–2835.

Figure 6. FESEM images of oriented rutile TiO_2 nanorod films grown from a two-step hydrothermal reaction; (a) and (b) with and (c) and (d) without addition of saturated aqueous NaCl solution.
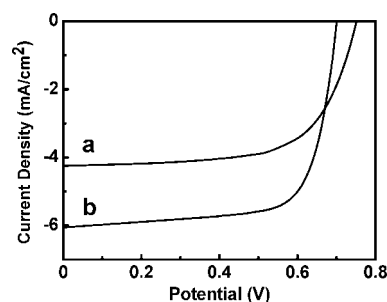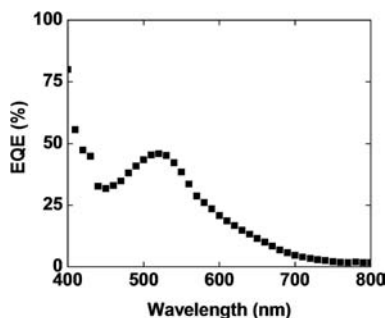

Figure 7. Photocurrent−photovoltage characteristics of a DSSC assembled from a 4 μm long rutile TiO_2 nanorod film (a) without and (b) with $TiCl_4$ treatment.

Cl^- could preferentially adsorb and retard the growth rate of (110) surfaces.[14]

The ability to retard the diameter growth rate through salt addition helps grow longer TiO_2 nanorods while avoiding the side surfaces from coalescing to form a continuous film. This is achieved through a two-step hydrothermal growth process (Figure 6). In the first step, TiO_2 nanorods were grown on FTO substrate at 200 °C for 4 h. In the second step, the FTO substrate obtained from step 1 was moved to another reaction vessel filled with freshly prepared growth solution that included NaCl. Hydrothermal growth was continued in this solution at 150 °C for 20 h to complete the nanorod growth. During this second growth period, the nanorods grow taller but the diameter remains unchanged. In control experiments, when no NaCl is added to the solution in the second step of the growth, the nanorods grow taller and wider, ultimately touching each other to form a continuous film with large grains at the bottom.

An FTO substrate covered with 4 μm long TiO_2 nanorods was used as the photoanode in assembling a DSSC. The current−voltage characteristic and the EQE of a typical cell are shown in Figures 7 and 8, respectively. Under 100 mW cm^{-2} of AM1.5 illumination, the $TiCl_4$-treated cell exhibits a short circuit current of $\sim$6.05 mA cm^{-2}, an open circuit voltage of $\sim$0.71 V, and a fill factor of 0.7. The EQE is $\sim$50% at the peak of the dye absorption. The overall power conversion efficiency was found to be 3.0%. Considering the length of the

Figure 8. External quantum efficiency (EQE) of a DSSC assembled from 4 μm long nanorods treated with TiCl$_4$.

nanorods, ~4 μm, higher efficiencies could be achieved with longer nanorods.

Roughness factor of the TiO$_2$ photoanodes were estimated by desorbing the dye and measuring the absorption of the dye solution. Using a dye adsorption area of 1.6 nm^2 we estimate a roughness factor of ~200 for TiCl$_4$-treated nanorods. The beneficial effects of TiCl$_4$ treatment is well-known in TiO$_2$ nanoparticle cells.[5,27,28] One of these reasons that is operative in nanoparticle DSSCs is the formation of a blocking TiO$_2$ layer on the uncovered regions of the FTO to reduce the shunt current; this improves the fill factor. Improved fill factor indicates that this may also be the case in nanorod-based DSSCs. Moreover, the roughness factor of nanorods is ~150 without TiCl$_4$ treatment, indicating that at least one other role of this treatment is to increase dye adsorption, either by increasing the nanoscopic roughness of the nanorods or by clearing the surface of molecules that may compete with dye adsorption. The TiCl$_4$ treatment can also decrease surface recombination, but dye desorption measurements indicate that the observed improvement is due to increased dye adsorption and optical density of the photoanode. If TiCl$_4$ treatment roughens the nanorod surfaces, this effect is too small to see by electron microscopy but is measurable by dye desorption. An estimate of the roughness factor from nanorod density and dimensions measured by SEM (4 μm long, 90 nm in diameter, and 40 nanowires/μm^{-2}) gives roughness factors that are on the order of 50, a factor of 3−4 lower than that measured by dye desorption.

However, roughness factor estimation from nanowire areal density measured at the end of the growth may be misleading because the nanorods are denser during the initial stages of growth and their areal density is reduced as those that are growing at an angle to the surface normal run into neighboring rods and stop. This effect was quantified in ZnO nanowire growth, and a factor of 5 loss in nanowire density is possible through this mechanism.[3] Thus, the nanowire density at the beginning stages of the growth may be much higher (~100−200 μm^{-2}) than that determined at the end of the growth (~40 μm^{-2}).

Conclusions

In summary, a facile hydrothermal method was developed for the first time to grow oriented single-crystalline rutile TiO$_2$ nanorod films on transparent conductive substrates. The growth parameters including the growth time, the growth temperature, the initial reactant concentration, acidity, and types of additives could be selectively chosen to prepare TiO$_2$ nanorod film with desired lengths and densities. The small lattice mismatch between the FTO substrate and rutile TiO$_2$ plays a key role in driving the nucleation and growth of the rutile TiO$_2$ nanorods on FTO. With TiCl$_4$-treatment, a light to electricity conversion efficiency of 3% could be reached by employing a 4-μm long TiO$_2$ nanorod film as the photoanode in a DSSC. Further improvements in the cell efficiency should be possible with longer nanorods.

Note Added in Proof. After submission of this article a different method that also yields TiO$_2$ nanowires on transparent conducting oxide substrates has been published.[29]

Supporting Information Available: EDX and FESEM results for oriented TiO$_2$ nanorods (PDF). This material is available free of charge via the Internet at http://pubs.acs.org.

JA8078972

(27) Sommeling, P. M.; O'Regan, B. C.; Haswell, R. R.; Smit, H. J. P.; Bakker, N. J.; Smits, J. J. T.; Kroon, J. M.; van Roosmalen, J. A. M. *J. Phys. Chem. B* **2006**, *110*, 19191–19197.

(28) Zhu, K.; Schiff, E. A.; Park, N.-G.; van de Lagemaat, J.; Frank, A. J. *Appl. Phys. Lett.* **2002**, *80*, 685–687.

(29) Feng, X.; Shankar, K.; Varghese, O. K.; Paulose, M.; Latempa, T. J.; Grimes, C. A. *Nano Lett.* **2008**, *8*, 3781–3786.